*Engineering Transactions*, **72**(1): 39–60, 2024, doi: 10.24423/EngTrans.3206.2024
Institute of Fundamental Technological Research Polish Academy of Sciences (IPPT PAN)
Université de Lorraine • Poznan University of Technology

# Research Paper

## Green Fibers-Reinforced Cement Mortar with the Inclusion of Nano-$CaCO_3$ and Metakaolin

Ali Jihad HAMAD[1)*], Rami Joseph SLDOZIAN[2)], Ruqaya F. KADHIM[2)]

[1)] *Department of Building and Construction Engineering*
*Engineering Technical College of Mosul, Northern Technical University*
41002, Mosul, Iraq; e-mail: ali.j.hamad@ntu.edu.edu

[2)] *Department of Applied Sciences, University of Technology*
Baghdad, Iraq; e-mail: 100385@uotechnology.edu.iq, ruqay.f.kadhim@uotechnology.edu.iq

[*]Corresponding Author e-mail: alijihadengineer@yahoo.com

Over the previous few decades, there has been a noticeable increase in interest in the use of vegetable fibers and supplemental cementitious elements in mortar and concrete. The date palm frond was utilized in this study to create date palm fibers (DPF), which were then added to the cement mortar at percentages of 1%, 2%, 3%, 4%, and 5% by cement weight. There were two types of DPFs used: one type was untreated, and the other had a mechanical treatment that created holes before applying a layer of polychloroprene (neoprene) on the surface. Metakaolin (MK) and nano calcium carbonate (nano-$CaCO_3$) were added to the cement mortar by the weight of cement. MK was replaced by 10% of the weight of cement. Besides, the nano-$CaCO_3$ was replaced by 1%, 2%, 3%, and 4% of the weight of cement. Mechanical tests for flowability, compressive strength, and flexural strength were conducted. In addition, one MCDM methodology called VIKOR is utilized to choose the best combination out of several combinations and criteria. The results indicate that a higher DPF concentration enhances both compressive and flexural strength. The mixtures with the DPF coating and mechanical treatment give the strongest and most significant results. In addition, the flowability of cement mortar decreases when the DPF concentration increases. In addition to the high content of nano-$CaCO_3$ in cement mortar, given the grater reading of strength, the presence of nano-$CaCO_3$ in cement mortar reduces the disparity in result values that have a higher DPF content. The mixtures containing 4% and 5% DPF and 3% and 4% nano-$CaCO_3$ are the optimal ones, according to the VIKOR technique.

**Keywords:** fibers reinforced cement mortar; date palm fibers (DPF); nano calcium carbonate (nano-$CaCO_3$), metakaolin (MK); pozzolanic materials.

## 1. Introduction

There has been a significant surge of interest in the incorporation of supplementary cementitious materials such as silica fume, fly ash, and metakaolin in concrete based on ordinary Portland cement (OPC) over the past few decades [1–7]. The utilization of this technology presents an effective approach to reducing the carbon footprint of concrete by minimizing the amount of ordinary OPC used. Incorporating supplementary cementitious materials (SCMs) in place of OPC offers potential benefits, including improved mechanical properties and durability [8–13]. Metakaolin, a representative supplementary cementitious material derived from controlled calcination of kaolin clay, exhibits exceptional pozzolanic reactivity [14]. Partially replacing OPC with metakaolin in concrete leads to significant improvements in the mechanical properties. This is due to the increased production of binding material, calcium silicate hydrates (C-S-H), through the pozzolanic reaction between metakaolin and calcium hydroxide (CH). Furthermore, the extensive surface area of metakaolin provides more sites for OPC hydration, enhancing the overall hydration process [15]. While ground limestone is commonly considered an inert mineral filler due to its composition, which mainly consists of calcite ($CaCO_3$) and particle sizes similar to regular OPC [16], adding a significant amount of pulverized limestone to concrete can significantly reduce its strength due to dilution. However, incorporating a small quantity of crushed limestone can slightly increase the compressive strength of concrete, as the reactivity of limestone powders with the aluminate phases in OPC is limited [17, 18]. This reaction between aluminate phases and calcium carbonate in limestone produces and stabilizes ettringite, a hydration product with a larger volume compared to other OPC hydration products. As a result, the microstructure of the hardened concrete becomes denser, leading to higher compressive strength. Antoni et al. demonstrated that leveraging the synergistic effects between ground limestone and metakaolin can further improve the properties of metakaolin-blended cement-based concrete [19–22]. The inclusion of $CaCO_3$ can influence the distribution of lime, alumina, and sulfate within the concrete, thereby altering the mineralogy of the hydrated cement pastes [23, 24].

According to research by Balasubramanian and Selvan [25], the utilization of natural vegetable fibers in cement composites offers various advantages compared to fiberglass-reinforced components. These advantages include a 10% reduction in weight, an 80% reduction in energy consumption during production, and a 5% reduction in component costs. However, incorporating natural vegetable fibers into concrete has also been associated with certain disadvantages.

In 2018, Çomak *et al.* [26], determined that cement mortars reinforced with 2–3% amount and 12 mm length of natural hemp fiber give the optimum results, improving significantly performance in compressive strength, flexural strength, and splitting tensile strength. Besides, the effect of hemp fibers on the flow of fresh concrete is almost negligible.

Most natural vegetable fibers have a high water absorption capacity, which can lead to poor workability in fresh concrete and degradation in alkaline environments. Consequently, these factors can negatively affect desirable properties such as tensile strength and bond strength [27–33]. Nevertheless, researchers have proposed various treatments for these fibers, showing the potential to overcome these drawbacks [34–39]. Additionally, it has been argued that the high water absorption of natural vegetable fibers can be advantageous for the internal curing of the composite [40]. According to research by Lertwattanaruk and Suntijitto [41], the use of natural vegetable fiber-reinforced cement composites instead of asbestos cement composites offers significant advantages in terms of non-toxicity. This substitution eliminates the risks associated with human exposure to diseases such as asbestosis, cancer, malignant pleural disease, and tumors. In response to these health concerns, several countries have implemented legislation against the use of asbestos [42]. The study also emphasizes that the process of obtaining natural vegetable fibers is environmentally sustainable and free from pollution. Furthermore, since these fibers are widely available worldwide, they can be locally enhanced to suit specific climate requirements, reducing the need for material imports [43].

The aim of this work is to effectively create a sustainable cement mortar employing natural fibers (DPF). The research also emphasizes the use of modified and treated palm fronds. Furthermore, metakaolin was substituted by cement weight, and the pozzolanic material, represented bynano-$CaCO_3$, was used. The mechanical characteristics (compressive strength and flexural strength) of cement mortar reinforced with green fibers were investigated.

## 2. Experimental work

### *2.1. Materials*

Samples were prepared using a general-purpose cement-OPC, manufactured by Tasluga/Iraq. The chemical and physical analyses of the OPC are shown in Tables 1 and 2. Sample preparation process was conducted following ASTM C150 [44]. The fine aggregate (sand) used in this study was sourced from the Al-Akhdar Region in Karbala. Furthermore, the sieve analysis of the fine aggregate was conducted in accordance with ASTM C33 [45] and is presented in Table 3. MK was supplied from the Dwekhla region of Iraq, and Table 4 shows the composition of MK. Nano-$CaCO_3$ is added to the mixture as an additional ingredient in powder form, replacing the weight of cement with particles approximately 10–45 nm in size. The physical characteristics of nano-$CaCO_3$ are shown in Table 5.

**Table 1**. Chemical properties of Portland cement.

| Composition | Content [%] | Specification ASTM C150 [44] |
|---|---|---|
| CaO | 64.0 | – |
| SiO2 | 21.0 | – |
| $Al_2O_3$ | 5.00 | – |
| $Fe_2O_3$ | 2.60 | – |
| MgO | 2.22 | <6% |
| $SO_3$ | 2.38 | <3% |
| L.O.I. | 3.25 | <3% |
| Insoluble residue | 1.1 | ≤0.75% |
| Lime saturation factor, L.S.F. | 0.95 | 0.66–1.02 |
| Main compounds (Bogue's equations) | | |
| $C_3S$ | 57.50 | – |
| $C_2S$ | 14.30 | – |
| $C_3A$ | 8.70 | – |
| $C_4AF$ | 10.80 | – |

**Table 2**. Physical properties of Portland cement.

| Physical properties | | |
|---|---|---|
| Test | Results | ASTM C150 [44] |
| Initial setting time [min] | 119<br>295 | Not less than 45 min<br>Not more than 375 min |
| Fineness (Blaine) [$m^2$/kg] | 485 | Min. 280 $m^2$/kg |
| Compressive strength of 50 mm cubic mortar specimen [MPa]<br>3 days<br>7 days | <br>22.5<br>25.0 | <br>Min. 12 MPa<br>Min. 19 MPa |

**Table 3**. Sieve analysis of sand.

| Sieve size [mm] | Passing [%] | Passing [%], ASTM C33 [45] |
|---|---|---|
| 4.75 | 93 | 90–100 |
| 2.36 | 86 | 85–100 |
| 1.18 | 82 | 75–100 |
| 0.60 | 70 | 60–79 |
| 0.30 | 30 | 12–40 |
| 0.15 | 7 | 0–10 |

**Table 4**. Composition of MK.

| Compound | Percentage by mass |
|---|---|
| $SiO_2$ | 52–53 |
| $Al2O_3$ | 42–43 |
| CaO | 0.02–0.1 |
| $Fe_2O_3$ | 0.5–1 |
| MgO | 0–1.0 |
| $SO_3$ | 0–0.1 |
| $Na_2O$ | 0–0.05 |
| $K_2O$ | 0.4–1.5 |

**Table 5**. Physical properties of nano-$CaCO_3$.

| Properties | Values |
|---|---|
| Morphology | Cubic or hexagonal |
| Color | White |
| pH | Not applicable |
| Bulk density [g/mL] | 0.68 |
| True density [g/cm$^3$] | 2.9 |
| Specific surface area [g/m$^2$] | 30–60 |
| Average particle size [nm] | 10–45 nm |
| Purity [%] | 97 |
| Melting point | 825 |
| Boiling point [°C] | Decomposes |
| Molecular weight [g/mol] | 100.09 |

### *2.2. Preparation of palm frond fibers*

DPFs are used as natural fibers sourced from palm trees. The properties of DPF are shown in Table 6. The frond palm is cut into many sizes, about 8–18 mm in length. The DPF was used in two ways: the first without any treatment of

**Table 6**. Properties of DPF.

| Properties | Values |
|---|---|
| Tensile strength [MPa] | $280 \pm 60$ |
| Density [g/cm$^3$] | 0.25–1.1 |
| Length [mm] | 8–18 |
| Diameter [µm] | 100–800 |

the DPF, and the second included a mechanical treatment where voids or holes were created in the DPF. The resulting fibers were placed in an oven at 80°C for 48 hours. Figure 1 demonstrates the mechanism of bonding between DPF and cement mortar.

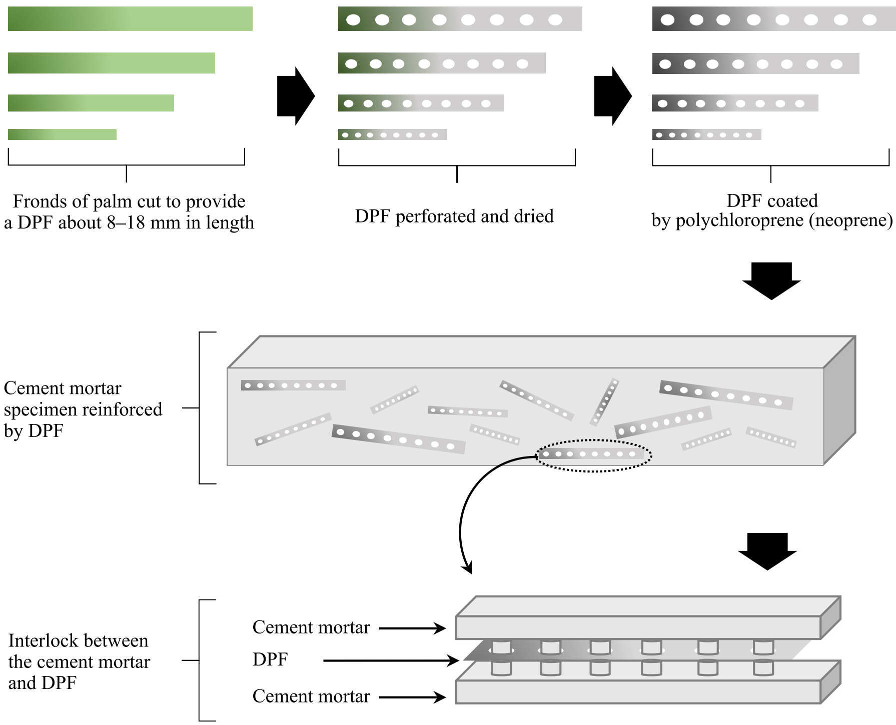


FIG. 1. The mechanism of bonding between DPF and cement mortar.

The DPF was coated or surface-treated with polychloroprene (neoprene), applied to the DPF surface as shown in Fig. 2. This rubber has a good balance of mechanical properties and fatigue resistance, which is second only to that of natural rubber but has superior oil, chemical, and heat resistance. Polychloroprene

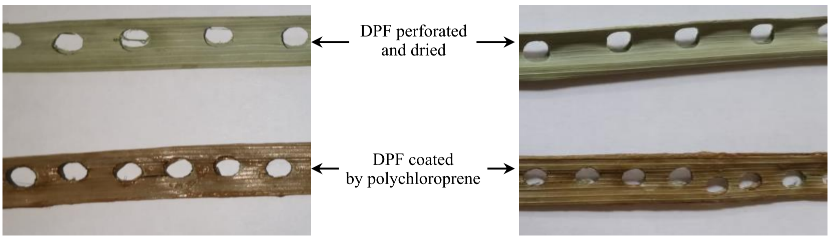


FIG. 2. The DPF perforated and coated surface by polychloroprene (neoprene).

exhibits excellent resistance to heat, ozone, weathering, and chemicals, making it highly durable. It also maintains flexibility over a wide temperature range, including both low and high temperatures. These properties make polychloroprene well-suited for various industrial and commercial applications. Neoprene is commonly used in the production of protective coatings, adhesives, gaskets, seals, and various types of rubber products. It is a popular choice in various industries due to its durability, flexibility, and chemical resistance, making it a preferred material in the production of wetsuits, gloves, and other items requiring water and abrasion resistance.

### *2.3. Mixing and preparation of specimens*

The mix proportion was 1:1, 0.45 (cement: sand, w/c = 0.45). Different fiber contents were added to the mortar mix. The DPF content was set at 1%, 2%, 3%, 4%, and 5% by weight of cement, as shown in Table 7. Cube molds of $50 \times 50 \times 50$ mm were cast for compressive strength testing in accordance with ASTM C109 [46]. Flexural strength tests were performed on $40 \times 40 \times 160$ mm beams subjected to the three-point flexural test in accordance with ASTM C348 [47]. A flow table test was performed to assess the workability of the mortar according to ASTM 1437 [48]. According to ASTM C192 [49], the specimen was stripped after 24 hours of casting and immersed in normal water at a limiting temperature of roughly $23 \pm 2°$C.

## 3. Results and discussion

### *3.1. Flowability*

The flowability of cement mortar reinforced by DPF, including MK and different contents of nano-$CaCO_3$ is assessed. The results of cement mortar reinforced with DPF are presented in Table 8. The control mix (M0) without DPF, MK, and nano-$CaCO_3$ revealed a flow value of 150%. Generally, the results exhibit a reduction in flowability with an increase in DPF content. This is attributed to the fact that the cement mortar matrix contained DPF that was dispersed randomly, worked as a skeleton, and finally hindered the flow of the cement mortar mixture [50–53]. Figure 3 shows the relationship between DPF content and flowability.

The lowest value of flow was 117% for mix M10 compared to the control mix. Alongside, it can be observed that the mixes containing coated DPF show higher flowability compared to the same mixes containing uncoated DPF. This is attributed to the smoother surface of DPF coated with neoprene, resulting in reduced friction with the cement mortar matrix. Additionally, nano-$CaCO_3$ and MK have an effect on flowability, which is contributed to higher surface

**Table 7**. Mix properties.

| Mixes | | | Mix proportions | DPF[a] [%] | MK[b] [%] | Nano-$CaCO_3$[c] [%] | Specimen no. of compressive strength | | Specimen no. of flexural strength | | Total no. of test specimens |
|---|---|---|---|---|---|---|---|---|---|---|---|
| | | | | | | | 7 days | 28 days | 7 days | 28 days | |
| Control mix | | M0 | 1:1, 0.45 (cement:sand, w/c = 0.45) | 0 | 0 | 0 | 3 | 3 | 3 | 3 | 12 |
| Uncoated | Without treatment | M1 | | 1 | 10 | 0 | 3 | 3 | 3 | 3 | 12 |
| | | M2 | | 2 | 10 | 1 | 3 | 3 | 3 | 3 | 12 |
| | | M3 | | 3 | 10 | 2 | 3 | 3 | 3 | 3 | 12 |
| | | M4 | | 4 | 10 | 3 | 3 | 3 | 3 | 3 | 12 |
| | | M5 | | 5 | 10 | 4 | 3 | 3 | 3 | 3 | 12 |
| | Mechanical treatment | M6 | | 1 | 10 | 0 | 3 | 3 | 3 | 3 | 12 |
| | | M7 | | 2 | 10 | 1 | 3 | 3 | 3 | 3 | 12 |
| | | M8 | | 3 | 10 | 2 | 3 | 3 | 3 | 3 | 12 |
| | | M9 | | 4 | 10 | 3 | 3 | 3 | 3 | 3 | 12 |
| | | M10 | | 5 | 10 | 4 | 3 | 3 | 3 | 3 | 12 |
| Coated by polychloroprene (neoprene) | Without treatment | M11 | | 1 | 10 | 0 | 3 | 3 | 3 | 3 | 12 |
| | | M12 | | 2 | 10 | 1 | 3 | 3 | 3 | 3 | 12 |
| | | M13 | | 3 | 10 | 2 | 3 | 3 | 3 | 3 | 12 |
| | | M14 | | 4 | 10 | 3 | 3 | 3 | 3 | 3 | 12 |
| | | M15 | | 5 | 10 | 4 | 3 | 3 | 3 | 3 | 12 |
| | Mechanical treatment | M16 | | 1 | 10 | 0 | 3 | 3 | 3 | 3 | 12 |
| | | M17 | | 2 | 10 | 1 | 3 | 3 | 3 | 3 | 12 |
| | | M18 | | 3 | 10 | 2 | 3 | 3 | 3 | 3 | 12 |
| | | M19 | | 4 | 10 | 3 | 3 | 3 | 3 | 3 | 12 |
| | | M20 | | 5 | 10 | 4 | 3 | 3 | 3 | 3 | 12 |
| Total no. of specimens | | | | | | | | | | | 252 |

[a] DPF added by weight of cement, [b] MK replaced by weight of cement, [c] Nano-$CaCO_3$ replaced by weight of cement.

**Table 8.** Results of the tests.

| Mixes | | | Mix proportions | DPF[a] [%] | MK[b] [%] | Nano-$CaCO_3$[c] [%] | Compressive strength [MPa] | | Flexural strength [MPa] | | Flowability [%] |
|---|---|---|---|---|---|---|---|---|---|---|---|
| | | | | | | | 7 days | 28 days | 7 days | 28 days | |
| Control mix | | M0 | 1:1, 0.45 (cement:sand, w/c = 0.45) | 0 | 0 | 0 | 24 | 32 | 4.5 | 6 | 150 |
| Uncoated | Without treatment | M1 | | 1 | 10 | 0 | 28 | 37 | 5.6 | 7.4 | 148 |
| | | M2 | | 2 | 10 | 1 | 30 | 40 | 6 | 8 | 143 |
| | | M3 | | 3 | 10 | 2 | 31 | 42 | 6.3 | 8.4 | 133 |
| | | M4 | | 4 | 10 | 3 | 31 | 42 | 6.3 | 8.4 | 125 |
| | | M5 | | 5 | 10 | 4 | 30 | 41 | 6.2 | 8.2 | 120 |
| | Mechanical treatment | M6 | | 1 | 10 | 0 | 28 | 38 | 5.7 | 7.6 | 145 |
| | | M7 | | 2 | 10 | 1 | 32 | 43 | 6.5 | 8.6 | 140 |
| | | M8 | | 3 | 10 | 2 | 33 | 45 | 6.8 | 9 | 138 |
| | | M9 | | 4 | 10 | 3 | 33 | 44 | 6.6 | 8.9 | 126 |
| | | M10 | | 5 | 10 | 4 | 33 | 44 | 6.6 | 9 | 117 |
| Coated by polychloroprene (neoprene) | Without treatment | M11 | | 1 | 10 | 0 | 30 | 40 | 6 | 8 | 150 |
| | | M12 | | 2 | 10 | 1 | 31 | 42 | 6.3 | 8.5 | 145 |
| | | M13 | | 3 | 10 | 2 | 33 | 45 | 6.8 | 9.1 | 138 |
| | | M14 | | 4 | 10 | 3 | 33 | 44 | 6.6 | 9.2 | 130 |
| | | M15 | | 5 | 10 | 4 | 35 | 47 | 7.1 | 9.4 | 125 |
| | Mechanical treatment | M16 | | 1 | 10 | 0 | 31 | 42 | 6.3 | 8.4 | 145 |
| | | M17 | | 2 | 10 | 1 | 33 | 44 | 6.6 | 8.9 | 142 |
| | | M18 | | 3 | 10 | 2 | 33 | 45 | 6.8 | 9.3 | 136 |
| | | M19 | | 4 | 10 | 3 | 35 | 47 | 7.1 | 9.6 | 127 |
| | | M20 | | 5 | 10 | 4 | 37 | 50 | 7.6 | 10 | 120 |

[a] DPF added by weight of cement, [b] MK replaced by weight of cement, [c] Nano-$CaCO_3$ replaced by weight of cement.

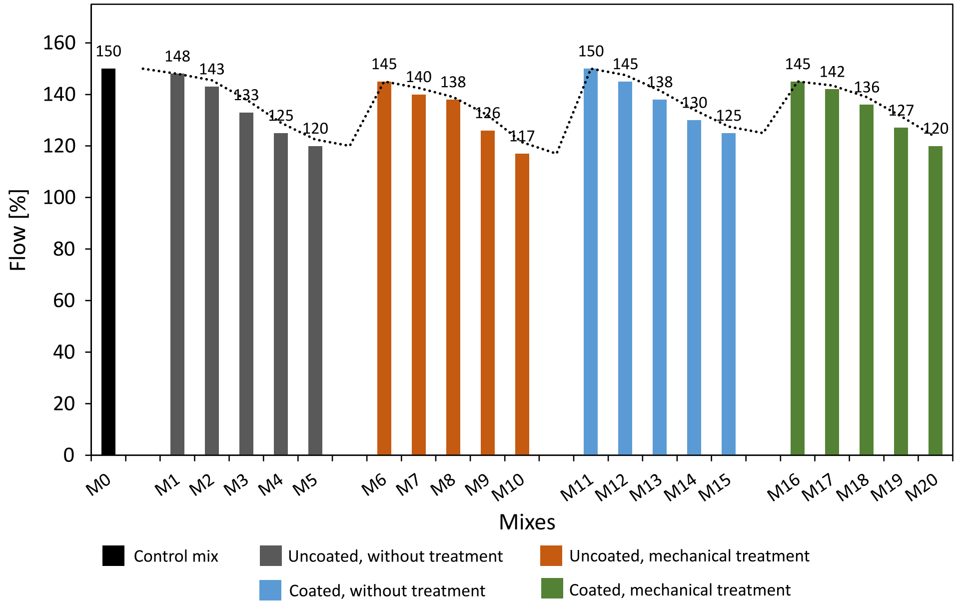


Fig. 3. Effect of DPF content on the flowability of cement mortar.

areas and finer particle sizes. Nanomaterials tend to absorb more water [54, 55], further increasing the cohesiveness of the cement mortar.

### *3.2. Compressive strength*

The compressive strength of cement mortar reinforced by DPF with different volume fractions of fibers and inclusion of MK and nano-$CaCO_3$ is presented in Table 8.

Figure 4 shows the effect of DPF on the compressive strength of cement mortar. It can be observed that the compressive strength is significantly influenced by the addition of DPF. The compressive strength increases with the rising content of DPF, and this increasing is attributed to the uniform distribution of DPF in the cement matrix [56, 57].

In Fig. 5, the mixes with perforated DPF exhibit significant results compared to others mixes. The highest increase in compressive strength is observed in mixes M19 and M20, containing 4% and 5% mechanically treated and coated DPF. Additionally, it can be observed the mixes with MK and high nano-$CaCO_3$ content show higher compressive strength. This is attributed to the increased contribution of hydration products, leading to increased compressive strength due to nano-$CaCO_3$, which in turn accelerates the C3A's reaction rate to produce carbon-aluminate [58–60].

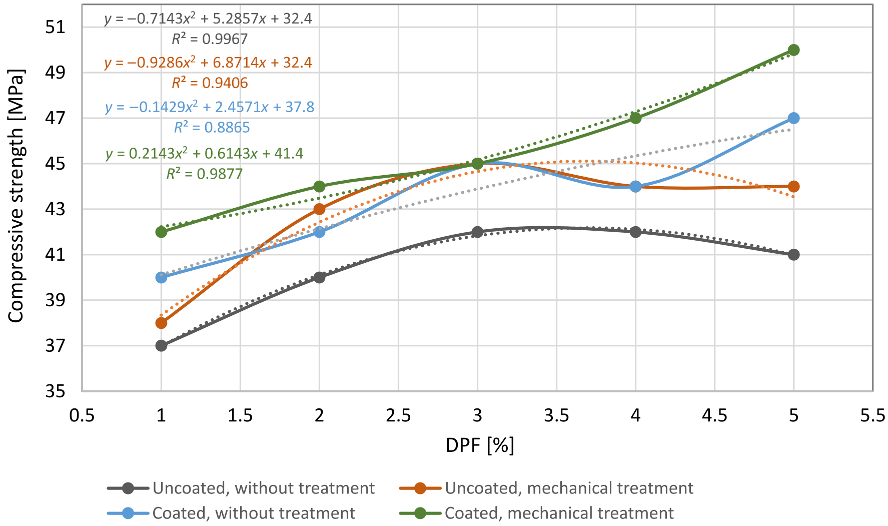


FIG. 4. Relationship between DPF content and compressive strength.

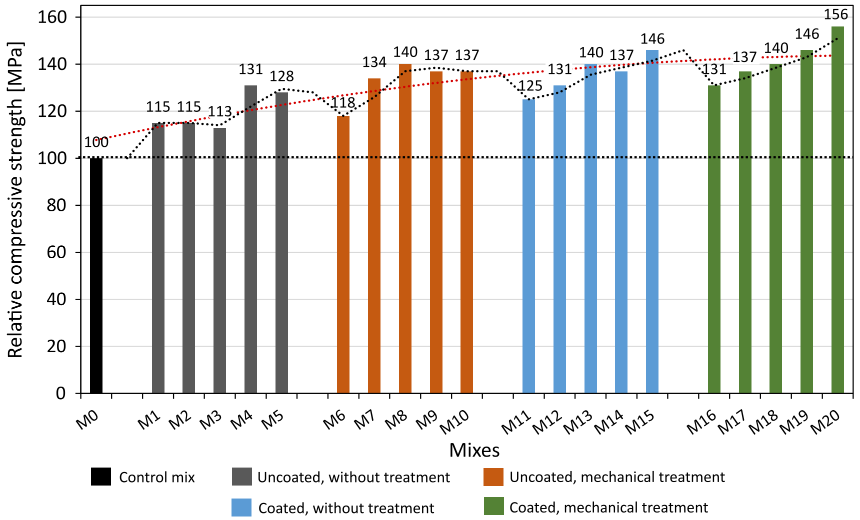


FIG. 5. Relative compressive strength of DPF reinforced cement mortar content.

## 3.3. *Flexural strength*

The flexural strength of cement mortar reinforced by DPF with different volume fractions of fibers and the inclusion of MK and nano-$CaCO_3$ are presented in Table 8.

Figure 6 shows the impact of DPF on the flexural strength of cement mortar. Flexural may be seen to have a major impact when the DPF is included. An in-

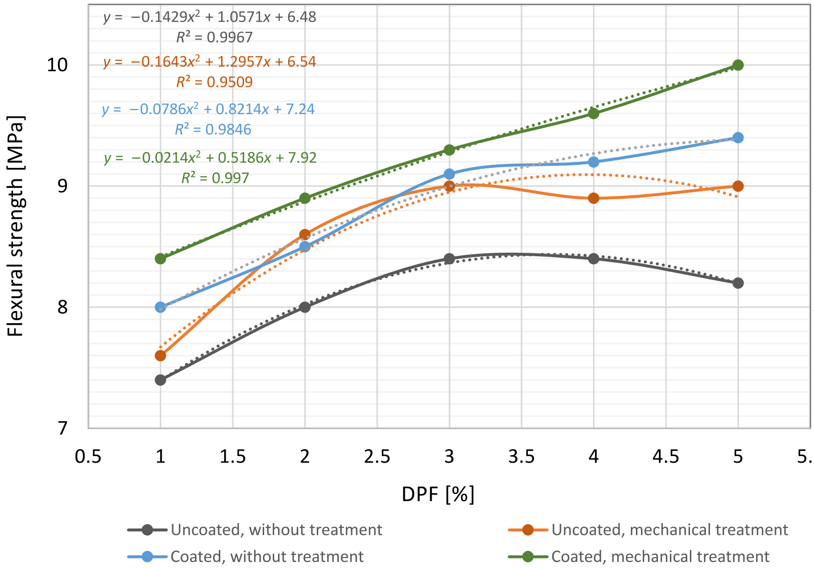


FIG. 6. Relationship between the flexural strength and DPF content.

crease in DPF concentration corresponds to an increase in flexural strength, attributed to the consistent distribution of DPF in the cement matrix [56, 57].

When compared to other mixtures, the mixes with perforated DPF exhibit interesting results. Figure 7 illustrates the increased flexural strength, partic-

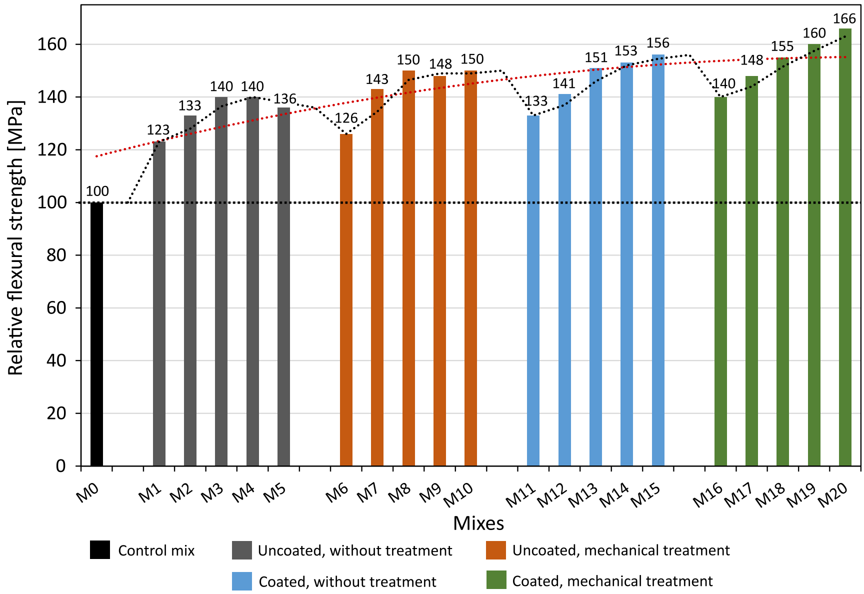


FIG. 7. Relative flexural strength of DPF-reinforced cement mortar content.

ularly notable in mixes M19 and M20, containing 4% and 5% mechanically treated and coated DPF. In addition, it is observed that mixes with high nano-$CaCO_3$ and MK content exhibit higher flexural strengths. This can be attributed to increased contributions from hydration products, which in turn boost strength due to nano-$CaCO_3$, which accelerates the rate at which C3A reacts to produce carbon-aluminate [58–62]. Figure 8 illustrates the mechanism of the bonding between the fibers and mortar, where the interlock between the mortar and the perforated DPF is apparent, showing the failure mode after applying flexural strength.


Fig. 8. Mechanism of bonding between the DPF and cement mortar (a), and the failure mode after applying flexural strength (b).

### *3.4. Vlsekriterijumska Optimizacija I Kompromisno Resenje (VIKOR)*

One of the multiple criteria decision making (MCDM) techniques is VIKOR (in English: *Multicriteria Optimization and Compromise Solution*) that evaluates options based on their proximity to the best possible solution and distance from the worst possible solution or negative ideal solution. The VIKOR technique involves multicriteria optimization of complex systems, with an emphasis on choosing and prioritizing options from a range of options when competing criteria are present. VIKOR determines a multicriteria raking index based on a specific measure of distance of each option to the optimal solution [63–65].

In this research, VIKOR was employed to find the optimal combination among various mixtures and criteria, considering factors such as needed strength, DPF fibers, and flowability. Conversely, the objective was to minimize the cost, density, certain fiber types, and cement content. Two types of criteria were considered: non-beneficial (minimum values are selected) and beneficial (maximum values that meet requirements are desired) [66–70]. The mathematical steps of VIKOR are outlined below:

**Step 1:** Find the best and worst values:

$$x_i^+ = \max x_{ij},$$

$$x_i^- = \min x_{ij},$$

where $i = 1, 2, 3, ..., m$; $j = 1, 2, 3, ..., n$.

**Step 2:** Normalization of $S_j$ and $R_j$:

$$S_j = \sum \left[ \frac{w_i(x_i^+ - x_{ij})}{x_i^+ - x_i^-} \right],$$

$$R_j = \max \left[ \frac{w_i(x_i^+ - x_{ij})}{x_i^+ - x_i^-} \right],$$

where $w_i$ is the weight of each criteria.

**Step 3:** Computation of $Q_j$:

$$Q_j = \frac{v(S_j - S^+)}{S_i^+ - S_i^-} + (1 - v) \left( \frac{R_j - R^+}{R^- - R^+} \right),$$

where the value of $v$ is usually equal to 0.5.

**Step 4:** Sort the values of $Q_j$ so that the lowest value, which represents a compromise, is the best option. This implies that a $Q_j$ rating value can be positioned higher the lower it is.

According to the results in Table 8, the candidate results are shown in Table 9, determining the best and worst values along with assigned weights for each criterion.

**Table 9**. Candidate results.

| Weight | 0.15 | 0.15 | 0.25 | 0.25 | 0.2 |
|---|---|---|---|---|---|
| Mix no. | DPF | Nano-$CaCO_3$ | Compressive strength | Flexural strength | Flowability |
| M0 | 0 | 0 | 32 | 6 | 150 |
| M1 | 1 | 0 | 37 | 7.4 | 148 |
| M2 | 2 | 1 | 40 | 8 | 143 |
| M3 | 3 | 2 | 42 | 8.4 | 133 |
| M4 | 4 | 3 | 42 | 8.4 | 125 |
| M5 | 5 | 4 | 41 | 8.2 | 120 |
| M6 | 1 | 0 | 38 | 7.6 | 145 |
| M7 | 2 | 1 | 43 | 8.6 | 140 |
| M8 | 3 | 2 | 45 | 9 | 138 |
| M9 | 4 | 3 | 44 | 8.9 | 126 |
| M10 | 5 | 4 | 44 | 9 | 117 |
| M11 | 1 | 0 | 40 | 8 | 150 |
| M12 | 2 | 1 | 42 | 8.5 | 145 |
| M13 | 3 | 2 | 45 | 9.1 | 138 |
| M14 | 4 | 3 | 44 | 9.2 | 130 |
| M15 | 5 | 4 | 47 | 9.4 | 125 |
| M16 | 1 | 0 | 42 | 8.4 | 145 |
| M17 | 2 | 1 | 44 | 8.9 | 142 |
| M18 | 3 | 2 | 45 | 9.3 | 136 |
| M19 | 4 | 3 | 47 | 9.6 | 127 |
| M20 | 5 | 4 | 50 | 10 | 120 |
| Best+ | 5 | 4 | 50 | 10 | 117 |
| Worst− | 0 | 0 | 32 | 6 | 150 |

Calculating $S_j$, $R_j$ and $Q_j$ and ranking the alternatives to obtain the optimal mixes are shown in Table 10.

The outcomes displayed in Table 10 are derived using the VIKOR method computation, where mix M20, which has the lowest score of 0, is ranked as the top option. Moreover, mix M15 is placed second.

## 4. Conclusion

According to the test results, several conclusions ca be drawn:

1) Cement mortar's flowability decreases when DPF content rises. Additionally, mechanical treatment of DPF resulted in the lowest flowability rating.

**Table 10**. Determining $S_j$, $R_j$ and $Q_j$.

| Mix no. | $S_j$ | $R_j$ | $Q_j$ | Rank of mixes |
|---|---|---|---|---|
| M0 | 0.85 | 0.2 | 1 | 21 |
| M1 | 0.685354 | 0.15 | 0.767424 | 20 |
| M2 | 0.531793 | 0.118182 | 0.590255 | 15 |
| M3 | 0.376616 | 0.088889 | 0.418896 | 12 |
| M4 | 0.272753 | 0.088889 | 0.356803 | 8 |
| M5 | 0.203636 | 0.1 | 0.345294 | 7 |
| M6 | 0.650606 | 0.15 | 0.746651 | 19 |
| M7 | 0.454823 | 0.1125 | 0.528997 | 14 |
| M8 | 0.33601 | 0.095455 | 0.412236 | 11 |
| M9 | 0.230076 | 0.066667 | 0.27167 | 5 |
| M10 | 0.116667 | 0.066667 | 0.203871 | 4 |
| M11 | 0.631111 | 0.15 | 0.734996 | 18 |
| M12 | 0.493662 | 0.127273 | 0.59185 | 16 |
| M13 | 0.33101 | 0.095455 | 0.409246 | 10 |
| M14 | 0.233258 | 0.066667 | 0.273572 | 6 |
| M15 | 0.099697 | 0.036364 | 0.112425 | 2 |
| M16 | 0.566162 | 0.15 | 0.696168 | 17 |
| M17 | 0.437803 | 0.113636 | 0.521871 | 13 |
| M18 | 0.311919 | 0.086364 | 0.373443 | 9 |
| M19 | 0.166288 | 0.045455 | 0.176625 | 3 |
| M20 | 0.013636 | 0.013636 | 0 | 1 |
| S+, R+ | 0.013636 | 0.013636 | | |
| S−, R− | 0.85 | 0.2 | | |

2) The compressive and flexural strengths are enhanced for mixtures with higher DPF concentrations. Given the significant results as compared to the control mix and other mixes, the mixes that employed mechanical DPF treatment were particularly noteworthy.
3) The addition of polychloroprene (neoprene)-coated DPF leads to a substantial increase in compressive and flexural strengths, with Mix M20 (containing approximately 5% DPF) showing an improvement of around 56% and 66%, respectively, compared to the control mix.
4) High nano-$CaCO_3$ content in cement mortar contributes to increased strength readings. The presence of nano-$CaCO_3$ helps reduce the variations in result values associated with higher DPF content.
5) According to the VIKOR technique, the mixtures containing 4% and 5% DPF, along with 3% and 4% nano-$CaCO_3$, are the optimal choices.

## References


1. Mehta P., High-performance, high-volume fly ash concrete for sustainable development, [in:] *Proceedings of the International Workshop on Sustainable Development and Concrete Technology*, Iowa State University Ames, IA, USA, pp. 3–14, 2004.

2. Ghrici M., Kenai S., Said-Mansour M., Mechanical properties and durability of mortar and concrete containing natural pozzolana and limestone blended cements, *Cement and Concrete Composites*, **29**(7): 542–549, 2007, doi: 10.1016/j.cemconcomp.2007.04.009.

3. Fairbairn E.M.R., Americano B.B., Cordeiro G.C., Paula T.P., Toledo Filho R.D., Silvoso M.M., Cement replacement by sugar cane bagasse ash: $CO_2$ emissions reduction and potential for carbon credits, *Journal of Environmental Management*, **91**(9): 1864–1871, 2010, doi: 10.1016/j.jenvman.2010.04.008.

4. Camiletti J., Soliman A.M., Nehdi M.L., Effects of nano- and micro-limestone addition on early-age properties of ultra-high-performance concrete, *Materials and Structures*, **46**: 881–898, 2013, doi: 10.1617/s11527-012-9940-0.

5. Haque M.N., Kayali O., Properties of high-strength concrete using a fine fly ash, *Cement and Concrete Research*, **28**(10): 1445–1452, 1998, doi: 10.1016/S0008-8846(98)00125-2.

6. Li G., Zhao X., Properties of concrete incorporating fly ash and ground granulated blast-furnace slag, *Cement and Concrete Composites*, **25**(3): 293–299, 2003, doi: 10.1016/S0958-9465(02)00058-6.

7. Li Z., Ding Z., Property improvement of Portland cement by incorporating with metakaolin and slag, *Cement and Concrete Research*, **33**(4): 579–584, 2003, doi: 10.1016/S0008-8846(02)01025-6.

8. Lothenbach B., Scrivener K., Hooton R.D., Supplementary cementitious materials, *Cement and Concrete Research*, **41**(12): 1244–1256, 2011, doi: 10.1016/j.cemconres.2010.12.001.

9. Sldozian R., Hamad A.J., Zayza M.J., Zeidan S.A., Thermal treatment influence of metakaolin on the concrete properties, *Journal of Pharmaceutical Negative Results*, **13**(Spec. Iss. 1): 1847–1855, 2022, doi: 10.47750/pnr.2022.13.S01.220.

10. Hamad A.J., Sldozian R.J.A., Mikhaleva Z.A., Effect of ceramic waste powder as partial fine aggregate replacement on properties of fiber-reinforced aerated concrete, *Engineering Reports*, **2**(3): e12134, 2020, doi: 10.1002/eng2.12134.

11. Aprianti E., A huge number of artificial waste material can be supplementary cementitious material (SCM) for concrete production – a review. Part II, *Journal of Cleaner Production*, **142**(4): 4178–4194, 2017, doi: 10.1016/j.jclepro.2015.12.115.

12. Sldozian R.J.A., Hamad A.J., Al-Rawe H.S., Mechanical properties of lightweight green concrete including nano calcium carbonate, *Journal of Building Pathology and Rehabilitation*, **8**(1): Article No 3, 2023, doi: 10.1007/s41024-022-00247-1.

13. Chandra Paul S., Mbewe P.B.K., Kong S.Y., Šavija B., Agricultural solid waste as source of supplementary cementitious materials in developing countries, *Materials*, **12**(7): 1112, 2019, doi: 10.3390/ma12071112.

14. Sabir B.B., Wild S., Bai J., Metakaolin and calcined clays as pozzolans for concrete: a review, *Cement and Concrete Composites*, **23**(6): 441–454, 2001, doi: 10.1016/S0958-9465(00)00092-5.

15. Siddique R., Klaus J., Influence of metakaolin on the properties of mortar and concrete: A review, *Applied Clay Science*, **43**(3–4): 392–400, 2009, doi: 10.1016/j.clay.2008.11.007.

16. Malhotra V.M., Carette G.G., Performance of concrete incorporating limestone dust as partial replacement for sand, *ACI Journal Proceedings*, **82**(3): 363–371, 1985, doi: 10.14359/10344.

17. Celik K., Jackson M.D., Mancio M., Meral C., Emwas A.-H., Mehta P.K., Monteiro P.J.M., High-volume natural volcanic pozzolan and limestone powder as partial replacements for Portland cement in self-compacting and sustainable concrete, *Cement and Concrete Composites*, **45**: 136–147, 2014, doi: 10.1016/j.cemconcomp.2013.09.003.

18. Senhadji Y., Escadeillas G., Mouli M., Khelafi H., Benosman, Influence of natural pozzolan, silica fume and limestone fine on strength, acid resistance and microstructure of mortar, *Powder technology*, **254**: 314–323, 2014, doi: 10.1016/j.powtec.2014.01.046.

19. Le Saoût G., Lothenbach B., Hori A., Higuchi T., Winnefeld F., Hydration of Portland cement with additions of calcium sulfoaluminates, *Cement and Concrete Research*, **43**: 81–94, 2013, doi: 10.1016/j.cemconres.2012.10.011.

20. Martin L.H.J., Winnefeld F., Müller C.J., Lothenbach B., Contribution of limestone to the hydration of calcium sulfoaluminate cement, *Cement and Concrete Composites*, **62**: 204–211, 2015, doi: 10.1016/j.cemconcomp.2015.07.005.

21. Antoni M., Rossen J., Martirena F., Scrivener K., Cement substitution by a combination of metakaolin and limestone, *Cement and Concrete Research*, **42**(12): 1579–1589, 2012, doi: 10.1016/j.cemconres.2012.09.006.

22. Nwa-David C.D., Onwuka D.O., Njoku F.C., Ibearugbulem O.M., Prediction of fresh and hardened properties of concrete containing nanostructured cassava peel ash using Ibearugbulem's approach, *Engineering and Technology Journal*, **41**(5): 652–665, 2023, doi: 10.30684/etj.2023.138099.1374.

23. Bentz D.P., Modeling the influence of limestone filler on cement hydration using CEMHYD3D, *Cement and Concrete Composites*, **28**(2): 124–129, 2006, doi: 10.1016/j.cemconcomp.2005.10.006.

24. Cui K., Lau D., Zhang Y., Chang J., Mechanical properties and mechanism of nano-$CaCO_3$ enhanced sulphoaluminate cement-based reactive powder concrete, *Construction and Building Materials*, **309**: 125099, 2021, doi: 10.1016/j.conbuildmat.2021.125099.

25. Balasubramanian, Chandrashekaran J., Selvan S.S., Experimental investigation of natural fiber reinforced concrete in construction industry, *International Research Journal of Engineering and Technology*, **2**(1): 179–182, 2015.

26. Çomak B., Bideci A., Bideci Ö., Effects of hemp fibers on characteristics of cement based mortar, *Construction and Building Materials*, **169**: 794–799, 2018, doi: 10.1016/j.conbuildmat.2018.03.029.

27. Agopyan V., Savastano Jr. H., John V.M., Cincotto M.A., Developments on vegetable fibre–cement based materials in São Paulo, Brazil: an overview, *Cement and Concrete Composites*, **27**(5): 527–536, 2005, doi: 10.1016/j.cemconcomp.2004.09.004.

28. Page J., Khadraoui F., Boutouil M., Gomina M., Multi-physical properties of a structural concrete incorporating short flax fibers, *Construction and Building Materials*, **140**: 344–353, 2017, doi: 10.1016/j.conbuildmat.2017.02.124.

29. Onuaguluchi O., Banthia N., Plant-based natural fibre reinforced cement composites: A review, *Cement and Concrete Composites*, **68**: 96–108, 2016, doi: 10.1016/j.cemcon comp.2016.02.014.

30. Teo D.C.L., Mannan M.A., Kurian J.V., Flexural behaviour of reinforced lightweight concrete beams made with oil palm shell (OPS), *Journal of advanced concrete technology*, **4**(3): 459–468, 2006, doi: 10.3151/jact.4.459.

31. Salau M., Adegbite I., Ikponmwosa E., Characteristic strength of concrete column reinforced with bamboo strips, *Journal of Sustainable Development*, **5**(1): 133, 2012, doi: 10.5539/jsd.v5n1p133.

32. Jabbar Z., Khalil W., Sustainable high-performance concrete reinforced with hybrid steel waste fibers, *Engineering and Technology Journal*, **40**(11): 1412–1421, 2022, doi: 10.30684/etj.2021.131833.1063.

33. Sldozian R.J., Hamad A.J., Al-Saffar Z.H., Burakova A.V., Tkachev A.G., Cement mortar reinforced by date palm fibers and inclusion metakaolin, *International Journal of Sustainable Building Technology and Urban Development*, **14**(3): 348–360, 2023, doi: 10.22712/susb.20230026.

34. Snoeck D., Smetryns P.A., De Belie N., Improved multiple cracking and autogenous healing in cementitious materials by means of chemically-treated natural fibres, *Biosystems Engineering*, **139**: 87–99, 2015, doi: 10.1016/j.biosystemseng.2015.08.007.

35. Wei J., Meyer C., Improving degradation resistance of sisal fiber in concrete through fiber surface treatment, *Applied Surface Science*, **289**: 511–523, 2014, doi: 10.1016/j.apsusc. 2013.11.024.

36. Shinoj S., Visvanathan R., Panigrahi S., Kochubabu M., Oil palm fiber (OPF) and its composites: A review, *Industrial Crops and Products*, **33**(1): 7–22, 2011, doi: 10.1016/j.indcrop.2010.09.009.

37. Hashim F.S., Yussof H.W., Zahari M.A.K.M., Rahman R.A., Illias R.M., Physicochemical and morphological characterisation of the native and alkaline pre-treated fibre pressed oil palm frond for fermentable sugars production, *Chemical Engineering Transactions*, **56**: 1087–1092, 2017, doi: 10.3303/CET1756182.

38. Machaka M., Basha H., Abou Chakra H., Elkordi A., Alkali treatment of fan palm natural fibers for use in fiber reinforced concrete, *European Scientific Journal*, **10**(12): 186–195, 2014, https://eujournal.org/index.php/esj/article/view/3198.

39. Ozerkan N.G., Ahsan B., Mansour S., Iyengar S.R., Mechanical performance and durability of treated palm fiber reinforced mortars, *International Journal of Sustainable Built Environment*, **2**(2): 131–142, 2013, doi: 10.1016/j.ijsbe.2014.04.002.

40. Momoh E.O., Osofero A.I., Recent developments in the application of oil palm fibers in cement composites, *Frontiers of Structural and Civil Engineering*, **14**: 94–108, 2020, doi: 10.1007/s11709-019-0576-9.

41. Lertwattanaruk P., Suntijitto A., Properties of natural fiber cement materials containing coconut coir and oil palm fibers for residential building applications, *Construction and Building Materials*, **94**: 664–669, 2015, doi: 10.1016/j.conbuildmat.2015.07.154.

42. Coutts R.S.P., A review of Australian research into natural fibre cement composites, *Cement and Concrete Composites*, **27**(5): 518–526, 2005, doi: 10.1016/j.cemconcomp.2004.09.003.

43. Javadian A., Wielopolski M., Smith I.F.C., Hebel D.E., Bond-behavior study of newly developed bamboo-composite reinforcement in concrete, *Construction and Building Materials*, **122**: 110–117, 2016, doi: 10.1016/j.conbuildmat.2016.06.084.

44. ASTM C150, *Specification for Portland Cement*, American Society for Testing and Materials, 2017.

45. ASTM C33 / C33M, *Standard Specification for Concrete Aggregates*, West Conshohocken, PA: ASTM International, 2017.

46. ASTM C109, *Standard Test Method for Compressive Strength of Hydraulic Cement Mortars (using 2-in. [50 mm] cube specimens)*, American Society of Testing and Materials, 2005.

47. ASTM C348, *Standard Test Method for Flexural Strength of Hydraulic-Cement Mortars*, ASTM C348-02, Annu book ASTM Stand 04.01, 2017.

48. ASTM C1437 / C1437M, *Standard Test Method for Flow of Hydraulic Cement Mortar*, West Conshohocken, PA: ASTM International, 2017.

49. ASTM C192 / C192M, *Standard Practice for Making and Curing Concrete Test Specimens in the Laboratory*, West Conshohocken, PA: ASTM International, 2017.

50. Chen H., Qin R., Chow C.L., Lau D., Recycling thermoset plastic waste for manufacturing green cement mortar, *Cement and Concrete Composites*, **137**: 104922, 2023, doi: 10.1016/j.cemconcomp.2022.104922.

51. Martinie L., Rossi P., Roussel N., Rheology of fiber reinforced cementitious materials: classification and prediction. *Cement and Concrete Research*, **40**(2): 226–234, 2010, doi: 10.1016/j.cemconres.2009.08.032.

52. Hamad A.J., Lightweight concrete reinforced with polypropylene fibers, *International Journal of Advances in Applied Sciences*, **4**(2): 45–49, 2015, doi: 10.11591/ijaas.v4.i2.pp45-49.

53. Dawood E.T., Hamad A.J., Toughness behaviour of high-performance lightweight foamed concrete reinforced with hybrid fibres, *Structural Concrete*, **16**(4): 496–507, 2015, doi: 10.1002/suco.201400087.

54. Zhang P., Wang L., Wei H., Wang J., A critical review on effect of nanomaterials on workability and mechanical properties of high-performance concrete, *Advances in Civil Engineering*, **2021**: Article ID 8827124, 2021, doi: 10.1155/2021/8827124.

55. Abdalla J.A., Thomas B.S., Hawileh R.A., Yang J., Jindal B.B., Ariyachandra E., Influence of nano-$TiO_2$, nano-$Fe_2O_3$, nanoclay and nano-$CaCO_3$ on the properties of cement/geopolymer concrete, *Cleaner Materials*, **4**: 100061, 2022, doi: 10.1016/j.clema.2022.100061.

56. Chakraborty S., Kundu S.P., Roy A., Basak R.K., Adhikari B., Majumder S.B., Improvement of the mechanical properties of jute fibre reinforced cement mortar: A statistical approach, *Construction and Building Materials*, **38**: 776–784, 2013, doi: 10.1016/j.conbuildmat.2012.09.067.

57. Fonseca C.S., Silva M.F., Mendes R.F., Hein P.R.G., Zangiacomo A.L., Savastano Jr. H., Tonoli G.H.D., Jute fibers and micro/nanofibrils as reinforcement in extruded fiber-cement composites, *Construction and Building Materials*, **211**: 517–527, 2019, doi: 10.1016/j.conbuildmat.2019.03.236.

58. Yang H., Che Y., Effects of nano-$CaCO_3$/limestone composite particles on the hydration products and pore structure of cementitious materials, *Advances in Materials Science and Engineering*, **2018**: Article ID 5732352, 2018, doi: 10.1155/2018/5732352.

59. Supit S.W.M., Shaikh F.U.A., Effect of nano-$CaCO_3$ on compressive strength development of high volume fly ash mortars and concretes, *Journal of Advanced Concrete Technology*, **12**(6): 178–186, 2014, doi: 10.3151/jact.12.178.

60. Luan C., Zhou Y., Liu Y., Ren Z., Wang J., Yuan L., Du S., Zhou Z., Huang Y., Effects of nano-$SiO_2$, nano-$CaCO_3$ and nano-$TiO_2$ on properties and microstructure of the high content calcium silicate phase cement (HCSC), *Construction and Building Materials*, **314**(Part A): 125377, 2022, doi: 10.1016/j.conbuildmat.2021.125377.

61. Guo X., Pan X., Mechanical properties and mechanisms of fiber reinforced fly ash–steel slag based geopolymer mortar, *Construction and Building Materials*, **179**: 633–641, 2018, doi: 10.1016/j.conbuildmat.2018.05.198.

62. Dalalbashi A., Ghiassi B., Oliveira D.V., Freitas A., Fiber-to-mortar bond behavior in TRM composites: Effect of embedded length and fiber configuration, *Composites Part B: Engineering*, **152**: 43–57, 2018, doi: 10.1016/j.compositesb.2018.06.014.

63. Arif M., Suseno J.E., Isnanto R.R., Multi-criteria decision making with the VIKOR and SMARTER methods for optimal seller selection from several e-marketplaces, *E3S Web of Conferences*, **202**: 14002, 2020, doi: 10.1051/e3sconf/202020214002.

64. Tong L.I., Chen C.C., Wang C.H., Optimization of multi-response processes using the VIKOR method, *The International Journal of Advanced Manufacturing Technology*, **31**(11): 1049–1057, 2007, doi: 10.1007/s00170-005-0284-6.

65. Akram M., Muhiuddin G., Santos-García G., An enhanced VIKOR method for multi-criteria group decision-making with complex Fermatean fuzzy sets, *Mathematical Biosciences and Engineering*, **19**(7): 7201–7231, 2022, doi: 10.3934/mbe.2022340.

66. Jing S., Niu Z., Chang P., The application of VIKOR for the tool selection in lean management, *Journal of Intelligent Manufacturing*, **30**(8): 2901–2912, 2019, doi: 10.1007/s10845-015-1152-3.

67. Jato-Espino D., Castillo-Lopez E., Rodriguez-Hernandez J., Canteras-Jordana J.C., A review of application of multi-criteria decision making methods in construction, *Automation in Construction*, **45**: 151–162, 2014, doi: 10.1016/j.autcon.2014.05.013.

68. Chatterjee P., Chakraborty S., A comparative analysis of VIKOR method and its variants, *Decision Science Letters*, **5**(4): 469–486, 2016, doi: 10.5267/j.dsl.2016.5.004.

69. Jahan A., Mustapha F., Ismail M.Y., Sapuan S.M., Bahraminasab M., A comprehensive VIKOR method for material selection, *Materials & Design*, **32**(3): 1215–1221, 2011, doi: 10.1016/j.matdes.2010.10.015.

70. Chang C.L., A modified VIKOR method for multiple criteria analysis, *Environmental Monitoring and Assessment*, **168**(1): 339–344, 2010, doi: 10.1007/s10661-009-1117-0.

*Received November 13, 2023; accepted version January 5, 2024.*
*Online first February 13, 2024.*